FERROELECTRICS

1. Introduction

Polarization which can be induced in nonconducting materials by means of an externally applied electric field $\overline{E}$ is one of the most important parameters in the theory of insulators, which are called dielectrics when their polarizability is under consideration (1). Experimental investigations have shown that these materials can be divided into linear and nonlinear dielectrics in accordance with their behavior in a realizable range of the electric field. The electric polarization $\overline{P}$ of linear dielectrics depends linearly on the electric field $\overline{E}$, whereas that of nonlinear dielectrics is a nonlinear function of the electric field (2). The polarization values which can be measured in linear (normal) dielectrics upon application of experimentally attainable electric fields are usually small.

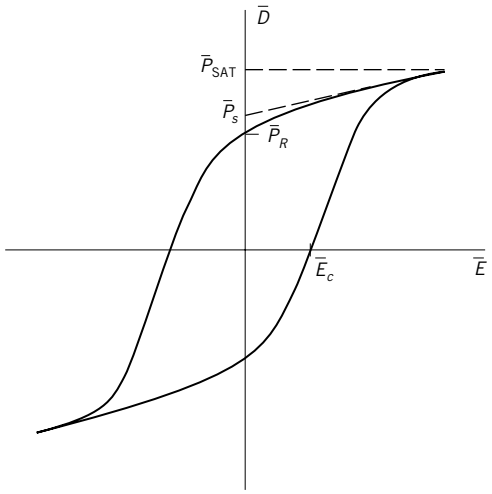

Fig. 1. Hysteresis loop of dielectric displacement, $\overline{D}$, versus applied electric field $\overline{E}$ where $\overline{E}_c$ is coercive field and $\overline{P}_{SAT}$, $\overline{P}_s$, and $\overline{P}_R$ are the saturated, spontaneous, and remanent polarization, respectively.

However, a certain group of nonlinear dielectrics exhibit polarization values which are several orders of magnitude larger than those observed in normal dielectrics (3). Consequently, a number of useful physical properties related to the polarization of the materials, such as elastic, thermal, optical, electromechanical, etc, are observed in these groups of nonlinear dielectrics (4).

The most important materials among nonlinear dielectrics are ferroelectrics which can exhibit a spontaneous polarization $\overline{P}_s$ in the absence of an external electric field and which can split into spontaneously polarized regions known as domains (5). It is evident that in the ferroelectric the domain states differ in orientation of spontaneous electric polarization, which are in equilibrium thermodynamically, and that the ferroelectric character is established when one domain state can be transformed to another by a suitably directed external electric field (6). It is the reorientability of the domain state polarizations that distinguishes ferroelectrics as a subgroup of materials from the 10-polar-point symmetry group of pyroelectric crystals (7–9).

Ferroelectric crystals exhibit spontaneous electric polarization and hysteresis effects in the relation between polarization and electric field, as shown in Figure 1. This behavior is usually observed in a limited temperature range, ie, usually below a transition temperature (10).

2. Properties

In considering the energy stored in a polarizable and deformable elastodielectric medium by separating the pure dielectric, pure elastic, and the cross-coupling terms, a phenomenological equation for the elastic Gibbs free energy may be

written in the simple form (4,11)

$$\Delta G_1 = \chi_{mn} P_m P_n + \text{higher order dielectric terms}$$

$$\frac{1}{2} s_{ijkl} T_{ij} T_{kl} + \text{higher order elastic terms}$$

$$-b_{mij} P_m T_{ij} - Q_{mnij} P_m P_n T_{ij} + \text{higher order cross terms}$$

where χ_{mn} = dielectric stiffness at constant elastic stress, P_m, P_n = components of the dielectric polarization, s_{ijkl} = elastic compliance at constant polarization, T_{ij}, T_{kl} = components of the elastic stress, b_{mij} = piezoelectric coefficient tensor (in polarization notation), and Q_{mnij} = electrostrictive coefficient tensor. Taking the partial derivatives of the energy function with respect to the different variables results in relations involving the quantities and properties of the material in terms of the coefficients of the energy function.

The dielectric stiffness c_{xij} can be expressed as a linear temperature dependence based on the Curie-Weiss law at above the Curie point T_c.

$$\chi_{ij} = \frac{1}{\epsilon_{ij}} = \chi_0 (T - T_c) = \frac{1}{C} (T - T_c)$$

or, solving for ε_{ij},

$$\epsilon_{ij} = \frac{C}{T - T_c}$$

where ϵ_{ij} = dielectric susceptibility , C = Curie constant, and T = temperature, which is similar to the susceptibility law for ferromagnets. However, for the dielectric case the Curie constant C is several orders of magnitude larger than that of the ferromagnet. In practice this means that very high useful dielectric permittivities persist for a wide range of temperature above T_c, ie, in the paraelectric phase. In fact, it is this high intrinsic dielectric susceptibility response that is the phenomenon most used in the practical application of polycrystalline ceramic ferroelectrics. Ferroelectric ceramics having relative permittivities $\epsilon_{ij}/\epsilon_0 = K_{ij}$ ranging up to 10,000, where ε_0 is the dielectric permittivity of vacuum, are widely used in many types of capacitors including the multilayer variety (see ADVANCED CERAMICS; CERAMICS; CERAMICS AS ELECTRICAL MATERIALS) (12).

The strain tensor S_{ij} can be written for noncentrosymmetry point group crystals as:

$$S_{ij} = s_{ijkl} T_{kl} + b_{ijm} P_m + Q_{mnij} P_m P_n$$

or for $T_{kl} = 0$,

$$S_{ij} = b_{ijm} P_m + Q_{mnij} P_m P_n$$

or

$$S_{ij} = d_{ijm} E_m + M_{nmij} E_m E_n$$

where d_{ijm} = the piezoelectric voltage coefficient tensor, M_{mnij} = the electrostrictive voltage coefficient tensor, and E_m and E_n = the electric field vectors. The piezoelectric and electrostrictive voltage coefficients, d_{ijm} and M_{mnij}, of the ferroelectronics are very large because of the large polarizability (13). Thus a second principal application of the ferroelectrics uses this high electromechanical coupling for efficient transduction between electrical and mechanical signals in sonic and ultrasonic transducers and filter applications.

Both the spontaneous polarization $\overline{P}_s$ and the remanent polarization $\overline{P}_R$ are strong functions of temperature, particularly near the transition temperature T_c in ferroelectrics (7):

$$\Delta\overline{P}_R = \pi\Delta T$$

where π is the pyroelectric coefficient. Many ferroelectrics have large pyroelectric coefficients and can be used in thermometry and in bolometry sensing devices of infrared radiation (see INFRARED TECHNOLOGY AND RAMAN SPECTROSCOPY; SENSORS).

Many ferroelectrics are high band gap insulating crystals and have good transparency in both the visible and near-ir spectral regions. Qualitatively, it may be expected that the large dielectric polarizability leads to an ability to modify the refractive index ellipsoid (indicatrix) under electric fields, thus resulting in high linear and quadratic electrooptic coefficients. Much research has been devoted to seeking to develop effective broad-band modulation and switching techniques for both bulk and thin-film materials by using ferroelectric electrooptic structures. Polycrystalline ceramic ferroelectrics have been processed to very high densities and good optical transparency (14). These materials possess new parameter combinations for modulation and imaging devices. Large photorefractive effects can also be generated in transparent ferroelectrics (15) (see CERAMICS, NONLINEAR OPTICAL AND ELECTROOPTIC CERAMICS).

In the single-domain state, many ferroelectric crystals also exhibit high optical nonlinearity and this, coupled with the large standing optical anisotropies (birefringences) that are often available, makes the ferroelectrics interesting candidates for phase-matched optical second harmonic generation (SHG).

One area of application utilizes the interaction between the dielectric polarization and the electrical transport processes in ferroelectrics. In single dielectric crystals the effects of the domain polarizations on the drift and retrapping of photogenerated carriers give most interesting photoferroelectric effects. Of more immediate applicability, however, are the large effects of the dielectric changes at the ferroelectric phase transition on the potential barriers at grain boundaries in suitably prepared semiconducting ceramic ferroelectrics. These barium titanate–based compositions show strong positive temperature coefficients of resistivity (PTC effects) and are finding widespread use in temperature and current control for domestic, industrial, and automotive applications.

3. Materials

3.1. Oxygen Octahedra. An important group of ferroelectrics is that known as the perovskites. The perfect perovskite structure is a simple cubic one

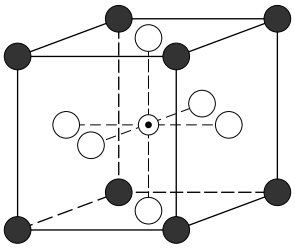

Fig. 2. Cubic (m3m) prototype structure of perovskite-type ABO_3 compounds where •, A; ⊙, B; and ç, O.

as shown in Figure 2, having the general formula ABO_3, where A is a monovalent or divalent metal such as Na, K, Rb, Ca, Sr, Ba, or Pb, and B is a tetra- or pentavalent cation such as Ti, Sn, Zr, Nb, Ta, or W. The first perovskite ferroelectric to be discovered was barium titanate [12047-27-7], and it is the most thoroughly investigated ferroelectric material (10).

Simple ABO_3 compounds in addition to $BaTiO_3$ are cadmium titanate [12014-14-1], $CdTiO_3$; lead titanate [12060-00-3], $PbTiO_3$; potassium niobate [12030-85-2], $KNbO_3$; sodium niobate [12034-09-2], $NaNbO_3$; silver niobate [12309-96-5], $AgNbO_3$; potassium iodate [7758-05-6], KIO_3; bismuth ferrate [12010-42-3], $BiFeO_3$; sodium tantalate, $NaTaO_3$; and lead zirconate [12060-01-4], $PbZrO_3$. The perovskite structure is also tolerant of a very wide range of multiple cation substitution on both A and B sites. Thus many more complex compounds have been found (16,17), eg, $(K_{1/2}B_{1/2})TiO_3$, $(Na_{1/2}Bi_{1/2})TiO_3$, $Pb(Sc_{1/2}Nb_{1/2})O_3$, $Pb(Fe_{1/2}Nb_{1/2})O_3$, and $Pb(Fe_{1/2}Ta_{1/2})O_3$.

The characteristic feature of the $BaTiO_3$ unit cell (Fig. 2) is the TiO_6-octahedron, which, because of its high polarizability, essentially determines the dielectric properties. The high polarizability results from the small Ti^{4+} ion having a relatively large space within the oxygen octahedron. The idealized unit-cell of Figure 2 where the Ti^{4+} ion is in the center of the oxygen octahedron is, however, stable only above the Curie point T_c of about 135°C. Below T_c the Ti^{4+} ions occupy off-center positions. This transition to the off-center position at T_c results in a series of important physical consequences (Fig. 3). The crystal structure changes from cubic ($T > 135$°C) via tetragonal (5°C $< T < 135$°C; $c/a = 1.01$) and orthorhombic (-90°C $< T < 5$°C) to rhombohedral ($T < -90$°C). At the same time a spontaneous polarization $\overline{P}_s$ (26 μC/cm^2 at room temperature) appears, the direction of which in the tetragonal phase is along one of the six edges, in the orthorhombic phase along one of the 12 surface diagonals, and in the rhombohedral phase along one of the eight body diagonals of the ideal cubic unit cell. The direction of $\overline{P}_s$ can be switched by a high (1–2 kV/cm) electrical field between the different crystallographically allowed and thermodynamically equilibrium positions which are characteristic in each ferroelectric phase (10,16).

At the temperatures of the phase transitions, maxima of the dielectric constant up to 10,000 are found. Moreover, in the ferroelectric state below T_c the material becomes pyroelectric and shows high piezoelectric activity.

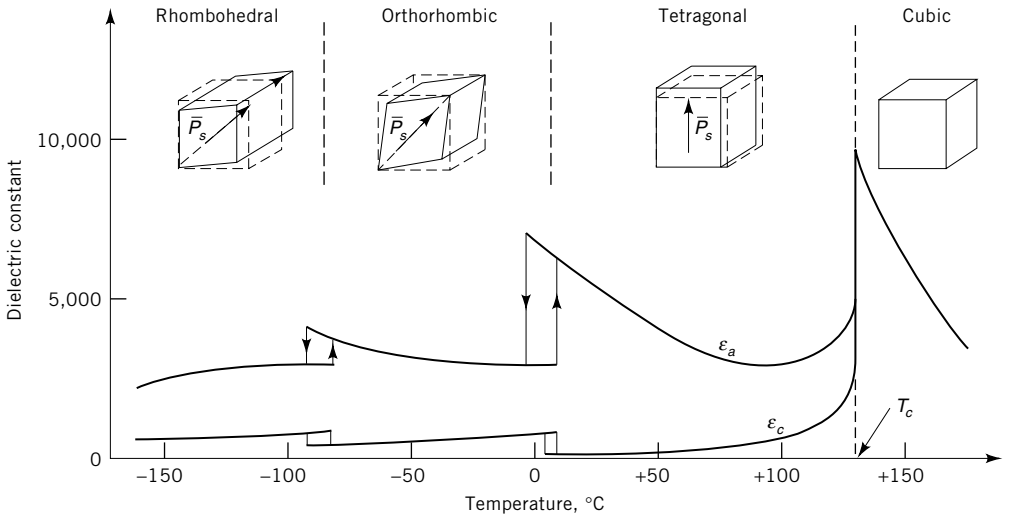

Fig. 3. Crystal structure and lattice distortion of the $BaTiO_3$ unit cell showing the direction of spontaneous polarization, and resultant dielectric constant ε vs temperature. The subscripts *a* and *c* relate to orientations parallel and perpendicular to the tetragonal axis, respectively. The Curie point, T_c, is also shown.

Perovskite-type compounds, especially $BaTiO_3$, have the ability to form extensive solid solutions. By this means a wide variety of materials having continuously changing electrical properties can be produced in the polycrystalline ceramic state. By substituting Pb^{2+} ions for Ba^{2+} ions, T_c can be increased linearly up to 490°C for a 100% Pb^{2+} substitution. In the same manner, T_c can be continuously decreased by the substitution of Sr^{2+} for Ba^{2+} or of Zr^{4+} or Sn^{4+} for Ti^{4+} (Fig. 4). Simultaneous with the change of T_c by formation of solid solutions, the low temperature phase transitions between tetragonal–orthorhombic and orthorhombic-rhombohedral phases shift in a rather complex manner.

3.2. $PbZrO_3$–$PbTiO_3$-Based Materials. Since the middle of the 1950s, solid solutions of $PbZrO_3$–$PbTiO_3$ (PZT) ceramics having the perovskite structure have gained rising interest because of the superior piezoelectric properties (10,17,18). The phase diagram of the $Pb(Zr_xTi_{1-x})O_3$ system is shown in Figure 5. At high temperatures, ie, above T_c, the ideal cubic paraelectric structure is stable and no ferroelectric phenomena such as spontaneous polarization appear. At room temperature the materials are ferroelectric and for Ti-rich compositions ($0 \leq x \leq 0.52$) show a tetragonal distortion of the unit cell. Compositions having lower ($0.52 \leq x \leq 0.94$) Ti content have rhombohedrally distorted unit cells. Both phases are separated by a morphotropic phase boundary at $x = 0.48$. Compositions near the Zr side of the system ($0.94 \leq x \leq 1$) are antiferroelectric and have orthorhombic structure. The direction of the spontaneous polarization $\bar{P}_s$ is along one of the edges of the unit cell for tetragonal distorted compositions and along one of the space diagonals for rhombohedral distorted compositions.

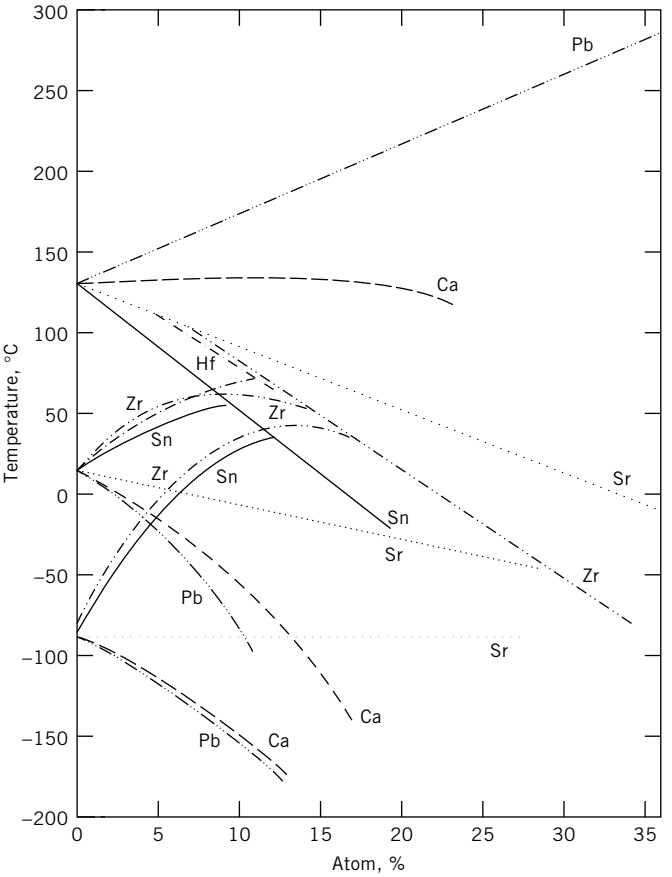

Fig. 4. Effect of isovalent substitutions on crystal structure transition temperatures of ceramic $BaTiO_3$ where (–·····) represents pb^{2+}; (– –), ca^{2+}; and (····) Sr^{2+}; substitution for Ba^{2+}; and (—) Sn^{4+}; (–·–·) Zr^{4+}; and (–··–) Hf^{4+}; substitution for Ti^{4+}. Transition temperatures for pure $BaTiO_3$ are 135, 15, and −90°C (see Fig. 3).

A third or even a fourth and fifth phase of a complex perovskite, for example, $Pb(Mg_{1/3}Nb_{2/3})O_3$, may be added in addition to $PbTiO_3$ and $PbZrO_3$ when forming the solid solution (10,19–21). In the same manner, 20 different elements having similar ionic radii can be substituted in place of Mg^{2+} or Nb^{4+}, leading to a huge number of possible combinations and a multitude of compositions which have, however, generally comparable properties. At low concentrations of a complex perovskite addition, the phase relationships of the quasibinary composition are maintained. Increasing amounts of a complex perovskite reduces T_c, and pseudocubic phases begin to appear.

There is often a wide range of crystalline solid solubility between endmember compositions. Additionally the ferroelectric and antiferroelectric Curie temperatures and consequent properties appear to mutate continuously with

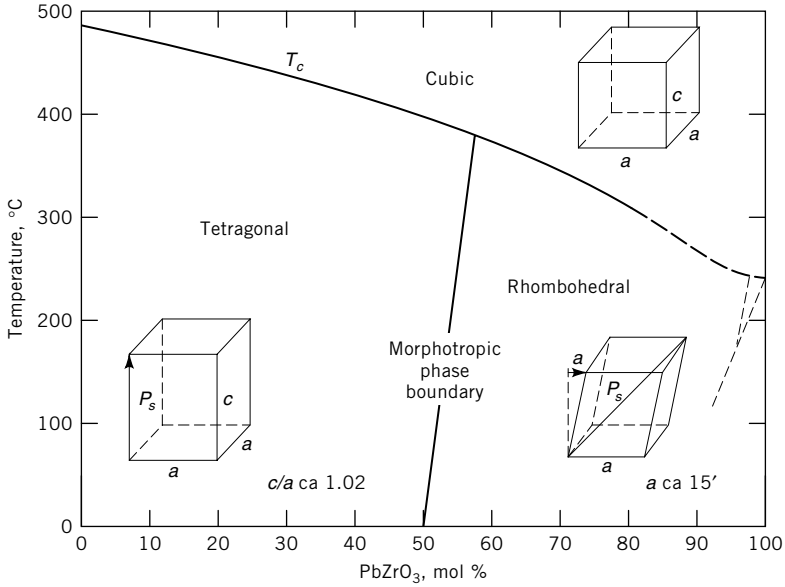

Fig. 5. Phase diagram of the $Pb(Zr_x, Ti_{1-x})O_3$ system.

fractional cation substitution. Thus the perovskite system has a variety of extremely useful properties. Other oxygen octahedra structure ferroelectrics such as lithium niobate [12031-63-9], $LiNbO_3$, lithium tantalate [12031-66-2], $LiTaO_3$, the tungsten bronze structures, bismuth oxide layer structures, pyrochlore structures, and order–disorder-type ferroelectrics are well discussed elsewhere (4,12,22,23).

4. Preparation of Ferroelectric Materials

4.1. Ceramics. The properties of ferroelectrics, basically determined by composition, are also affected by the microstructure of the densified body which depends on the fabrication method and condition. The ferroelectric ceramic process is comprised of the following steps (10,24,25): (*1*) selection of raw oxide materials, (*2*) preparation of a powder composition, (*3*) shaping, (*4*) densification, and (*5*) finishing.

Raw Materials. Most of the raw materials are oxides (PbO, TiO_2, ZrO_2) or carbonates ($BaCO_3$, $SrCO_3$, $CaCO_3$). The levels of certain impurities and particle size are specified by the chemical supplier. However, particle size and degree of aggregation are more difficult to specify. Because reactivity depends on particle size and the perfection of the crystals comprising the particles, the more detailed the specification, the more expensive the material. Thus raw materials are usually selected to meet application-dependent requirements.

Powder Preparation. Mixing. The most widely used mixing method is wet ball milling, which is a slow process, but it can be left unattended for the

whole procedure. A ball mill is a barrel that rotates on its axis and is partially filled with a grinding medium (usually of ceramic material) in the form of spheres, cylinders, or rods. It mixes the raw oxides, eliminates aggregates, and can reduce the particle size.

Calcination. Calcination involves a low ($< 1000°C$) temperature solid-state chemical reaction of the raw materials to form the desired final composition and structure such as perovskite for $BaTiO_3$ and PZT. It can be carried out by placing the mixed powders in crucibles in a batch or continuous kiln. A rotary kiln also can be used for this purpose to process continuously. A sufficiently uniform temperature has to be provided for the mixed oxides, because the thermal conductivity of powdered materials is always low.

Shaping. The calcined powders must be milled and a binder (usually organic materials) added if necessary for the forming procedure. Table 1 summarizes this procedure (25).

Densification. Sintering, hot-pressing, or hot-isostatic-pressing methods may be used to densify the shaped green ferroelectric ceramics to $\sim 95 - 100\%$ of theoretical value. Sintering takes place at high ($>1000°C$) temperatures for several hours. A green ferroelectric ceramic is converted into a denser structure of crystallite. The crystallites are joined to one another by grain boundaries the thickness of which vary from about 100 pm to over 1 μm. These usually consist of the second phase and have a great deal of influence on the electrical and mechanical properties of ferroelectric ceramic devices.

Grain growth which also affects the final properties occurs during the sintering. Using hot-isostatic-pressing (HIP) and hot-uniaxial-pressing (HUP), the ceramic density close to the theoretical value can be obtained. However, these latter processes are usually a little more expensive.

Finishing. The densified ferroelectric ceramic bodies usually require machining and metallizing for dimension and surface roughness control and electrical contact. Ceramic preparations are discussed in detail in the literature (10,25,26).

Table 1. **Ceramic Shaping Method**[a]

Shaping method	Type of feed material	Type of shape
dry pressing	free-flowing granules	small, simple shapes
isostatic pressing	fragile granules	larger, more intricate shapes
calendering	plastic mass based on an elastic polymer	thin plates
extrusion	plastic mass using a viscous polymer solution	elongated shapes of constant cross section
jiggering	stiff mud containing clay	large, simple shapes
injection molding	organic binder giving fluidity when hot	complex shapes
slip-casting	free-flowing cream	mainly hollow shapes
band-casting	free-flowing cream	thin plates and sheets
silk-screening	printing ink consistency	thin layers on substrates

[a]Ref. 25.

4.2. Thin-Film Ferroelectrics. The trends in integrated circuits (qv) and packaging technologies toward miniaturization have stimulated the development of ferroelectric thin films (27) (see PACKAGING, ELECTRONIC MATERIALS; THIN FILMS). Advances in thin-film growth processes offer the opportunity to utilize the material properties of ferroelectrics such as pyroelectricity, piezoelectricity, and electrooptic activity for useful device applications (28). The primary impetus of the activity in ferroelectric thin-film research is the large demand for the development of nonvolatile memory devices, also called FERRAMS (ferroelectric random access memories) (29). FERRAMS promise fast read and write cycles, low (3–5 V) switching voltages, nonvolatility, long (10^{12} cycles) endurance, and radiation hardness compatible with semiconductors (qv) such as gallium arsenide, GaAs (30).

Several techniques have been investigated for the preparation of ferroelectric thin films. The thin-film growth processes involving low energy bombardment include magnetron sputtering (31–34), ion beam sputtering (35,36), excimer laser ablation (37–39), electron cyclotron resonance (ECR) plasma-assisted growth (40,41), and plasma-enhanced chemical vapor deposition (PECVD) (42) (see PLASMA TECHNOLOGY). Other methods are sol-gel (43–45), metal organic decomposition (MOD) (46,47), thermal and *e*-beam evaporation (48,49), flash evaporation (50,51), chemical vapor deposition (CVD) (52), metal organic chemical vapor deposition (MOCVD) (53,54), and molecular beam epitaxy (MBE) (55).

The requirements of thin-film ferroelectrics are stoichiometry, phase formation, crystallization, and microstructural development for the various device applications. As of this writing multimagnetron sputtering (MMS) (56), multiion beam-reactive sputter (MIBERS) deposition (57), uv-excimer laser ablation (58), and electron cyclotron resonance (ECR) plasma-assisted growth (59) are the latest ferroelectric thin-film growth processes to satisfy the requirements.

4.3. Ferroelectric Ceramic–Polymer Composites. The motivation for the development of composite ferroelectric materials arose from the need for a combination of desirable properties that often cannot be obtained in single-phase materials. For example, in an electromechanical transducer, the piezoelectric sensitivity might be maximized and the density minimized to obtain a good acoustic matching with water, and the transducer made mechanically flexible to conform to a curved surface (see COMPOSITE MATERIALS, CERAMIC-MATRIX).

The development of active ceramic-polymer composites was undertaken for underwater hydrophones having hydrostatic piezoelectric coefficients larger than those of the commonly used lead zirconate titanate (PZT) ceramics (60–70). It has been demonstrated that certain composite hydrophone materials are two to three orders of magnitude more sensitive than PZT ceramics while satisfying such other requirements as pressure dependency of sensitivity. The idea of composite ferroelectrics has been extended to other applications such as ultrasonic transducers for acoustic imaging, thermistors having both negative and positive temperature coefficients of resistance, and active sound absorbers.

To optimize a ferroelectric ceramic and polymer composite device for a certain application, it is important to define a figure of merit which includes the most sensitive parameters. Maximizing a figure of merit requires not only choosing correct component phases having the right properties, but also designing the proper connectivity of the composite structures (60). Connectivity is a key feature

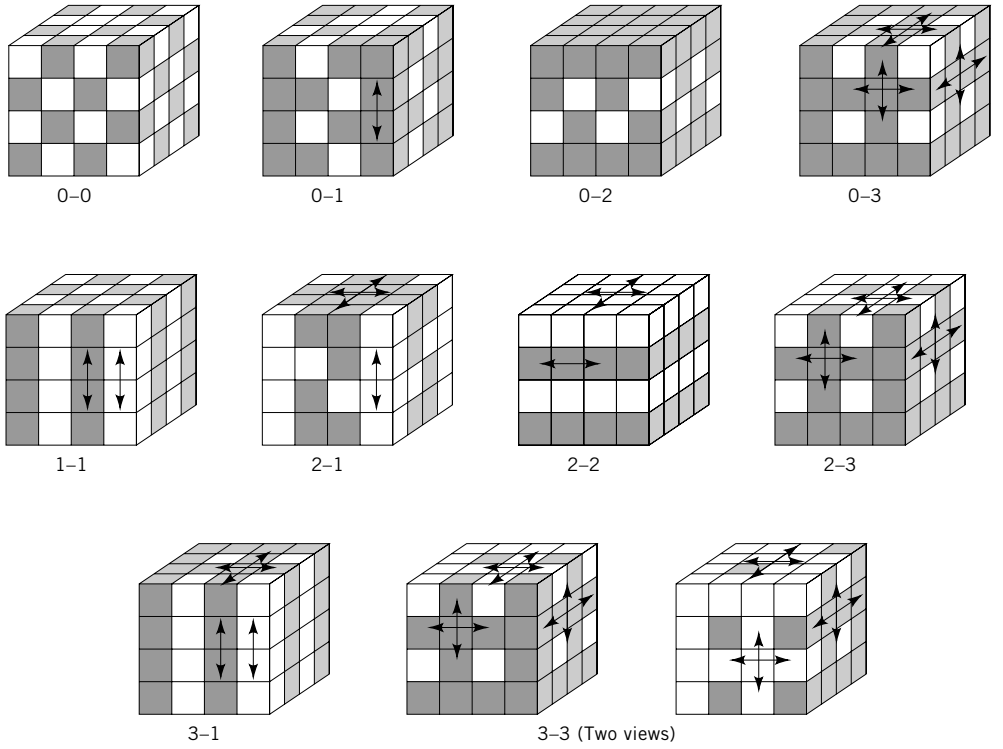

Fig. 6. Connectivity patterns for a diphasic solid showing zero-, one-, two-, or three-dimensional connectivity of each phase to itself. In the 3—1 composite, for instance, the shaded phase is three-dimensionally connected. Arrows are used to indicate the connected directions.

in property development in multiphase solids because physical properties can change by many orders of magnitude depending on the manner in which connections are made. Each phase in a composite may be self-connected in zero, one, two, or three dimensions. It is natural to confine attention to orthogonal systems. The 10 connectivity patterns for a diphase solid are shown in Figure 6. Extrusion, dicing, tape-casting, injection-molding, and hot-rolling methods are examples of processing techniques used for making ferroelectric composites having different connectivities. The 3—1 connectivity pattern is ideally suited to extrusion processing. A ceramic slip is extruded through a die giving a three-dimensionally connected pattern with one-dimensional holes, which can later be filled with a second phase.

5. Applications

5.1. Multilayer Capacitors. Multilayer capacitors (MLC), at greater than 30 billion units per year, outnumber any other ferroelectric device in production. Multilayer capacitors consist of alternating layers of dielectric material

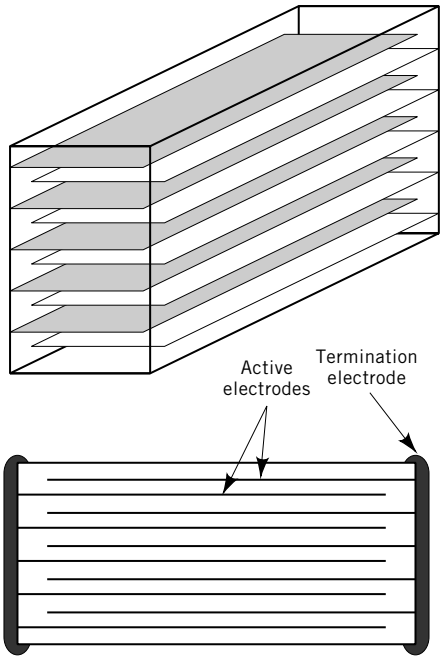

Fig. 7. Schematic of a conventional multilayer capacitor. The orientations of the internal and the termination electrodes are shown.

and metal electrodes, as shown in Figure 7. The reason for this configuration is miniaturization of the capacitor. Capacitance is given by

$$C = \frac{\epsilon_0 KA}{t}$$

where C is in Farads, ε_0 is permittivity in a vacuum, A is the area, K is the relative dielectric permittivity, and t is the thickness. Therefore, capacitance increases with increasing area and decreasing thickness. A multilayer capacitor usually contains up to 100 thin layers typically 10 to 35 μm thick of dielectric materials (26).

The dielectric materials used in multilayer capacitors must satisfy several electrical property requirements. A high dielectric permittivity with a minimal temperature dependence is desired for a wide temperature-range application of the MLC. $BaTiO_3$-based ceramics show high dielectric permittivities; however, the dielectric permittivity of $BaTiO_3$ ceramics has a strong temperature dependence and a maximum at the Curie point (Fig. 3). Although the Curie point can be shifted to room temperature by a partial substitution of Ba or Ti (Fig. 4), dielectric permittivity of $BaTiO_3$ ceramics also depends on the grain size of materials. When the powder is prevented from growing grains larger than 1.5 μm, the 90° domain walls are not formed. The material then remains stressed and the relative dielectric permittivity goes to $\sim 2500 - 3500$. Figure 8 compares

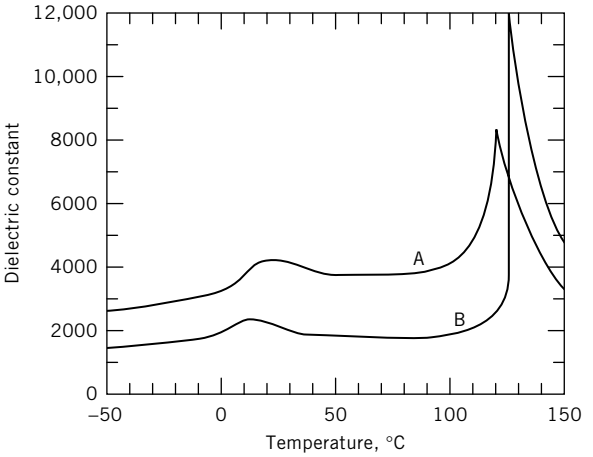

Fig. 8. Dielectric constant (1 kHz) vs temperature for $BaTiO_3$ ceramics of A, 1-μm grain size, and B, 50-μm grain size.

the dielectric constants vs temperatures of small- and large-grain undoped barium titanate (71).

5.2. Piezoelectric and Electrostrictive Device Applications. Devices made from ferroelectric materials utilizing their piezoelectric or electrostrictive properties range from gas igniters to ultrasonic cleaners (or welders) (72).

Applications of piezoelectric and electrostrictive ceramics include:

Classification	Applications
high voltage generators	gas appliances, cigarette lighters, fuses (igniters) for explosives, flash bulbs
high power ultrasonic generators	ultrasonic cleaners, sonar, echo sounding, ultra-sonic machining, atomization, pulverization
transducers for sound and ultrasound in air	microphones (eg, for telephones), burglar alarm systems, remote control, loudspeakers (eg, tweet-ers), buzzers, medical ultrasonics equipment
sensors	phonograph pick-ups, accelerometers, hydrophones, detection systems in machinery, musical instruments
resonators and filters	radios and televisions, remote control, electronic instrumentation
delay lines	color televisions, computers, electronic instrumen-tation
keyboards	computers, printers, desk calculators, vending machines, telephones
actuators	micropositioners, ink-jet printers
smart materials	active noise control for automobiles, aircraft, and trains; active shock absorber
electrooptic devices	optical shutter
composites	hydrophones, medical imaging transducers
miscellaneous	voltage transformers, flow meters

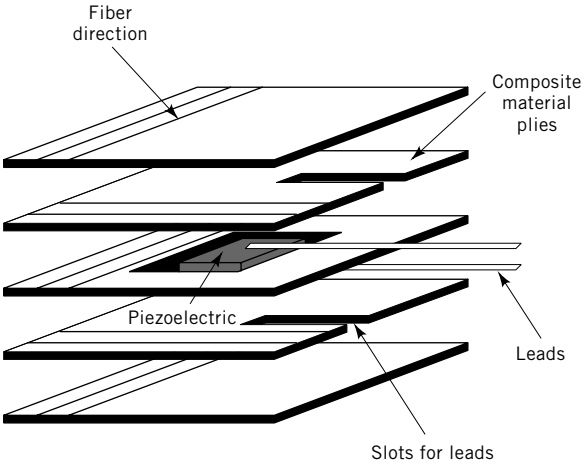

Fig. 9. Piezoelectric embedded inside a glass–epoxy laminate to form a composite smart structure.

Multilayer-type piezoelectric or electrostrictive actuators are used for several applications including the composite smart structure shown in Figure 9 (73).

Small ultrasonic motors such as the rotary actuator shown in Figure 10 have also been made and can be used for automobile windows, seats, and windshield wipers. Many small industrial motors could make use of the high torque, low speed, and precise stepping character of these actuators.

5.3. Composite Devices. Composites made of active-phase PZT and polymer-matrix phase are used for the hydrophone and medical imaging devices (see COMPOSITE MATERIALS, POLYMER-MATRIX; IMAGING TECHNOLOGY). A useful figure of merit for hydrophone materials is the product of hydrostatic strain coefficient d_h and hydrostatic voltage coefficient g_h where g_h is related to the d_h coefficient by (74)

$$g_h = d_h/\epsilon_0 \mathrm{K}$$

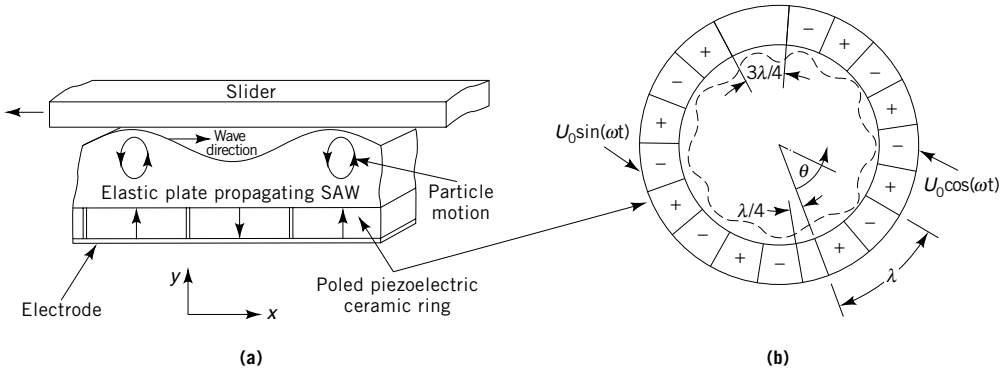

Fig. 10. The rotary actuator: (**a**) side view where SAW = surface acoustic wave; and (**b**) view of the poled piezoelectric ceramic ring showing poled segments and how temporal and spatial phase differences are established. Courtesy of Shinsei Kogyo Co.

Table 2. **Properties of Relaxor and Normal Ferroelectrics**[a]

Property	Normal ferroelectrics	Relaxor ferroelectrics
permittivity temperature dependence $\epsilon = \epsilon\,(T)$	sharp first- or second-order transition above Curie temperature	broad–diffuse phase transition about Curie maxima
permittivity temperature and frequency dependence $\epsilon = \epsilon\,(T,\varphi)$	weak frequency dependence	strong frequency dependence
remanent polarization	strong remanent polarization	weak remanent polarization
scattering of light	strong anisotropy (birefringent)	very weak anisotropy (pseudocubic)
diffraction of x-rays	line splitting owing to spontaneous deformation from paraelectric to ferroelectric phase	no x-ray splitting giving a pseudocubic structure

[a]Ref. 97.

Dielectric and piezoelectric properties of 3-3 type (60,63,75), 1–3 type (62,76–78), diced (79,80), 3–0 type (81,82), 3–1 and 3–2 type (83,84), and 0–3 type composites (69,85–88) have been investigated. For medical ultrasonic transducers, the 1–3 PZT rod and polymer composites are used. Electromechanical coupling properties of these materials are available (89–96).

5.4. Relaxor Ferroelectrics. The general characteristics distinguishing relaxor ferroelectrics, eg, the $PbMg_{1/3}Nb_{2/3}O_3$ family, from normal ferroelectrics such as $BaTiO_3$, are summarized in Table 2 (97). The dielectric response in the paraelectric-ferroelectric transition region is significantly more diffuse for the former. Maximum relative dielectric permittivities, referred to as K_{max}, are greater than 20,000. The temperature dependence of the dielectric properties is shown in Figure 11. The dielectric permittivity and loss exhibit dispersion near the

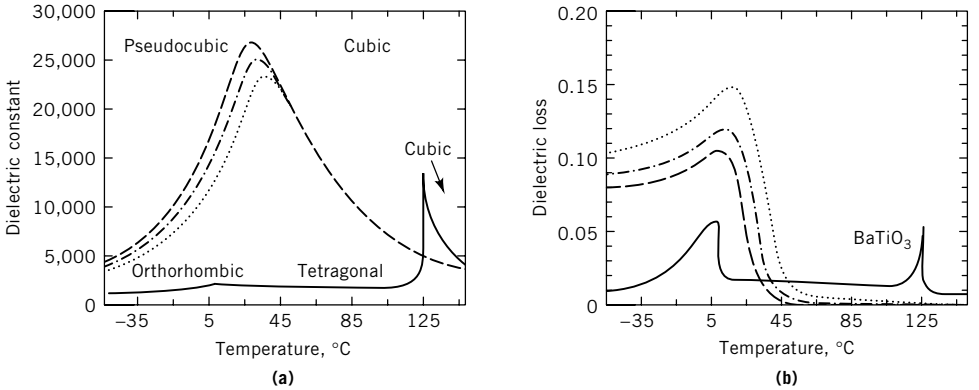

Fig. 11. Fundamental characteristics of relaxor materials compared to $BaTiO_3$. Temperature dependence for the relaxor ferroelectric 0.93 $PbMg_{1/3}Nb_{2/3}O_3$–0.07 $PbTiO_3$ at (– – –) 1, (–·–) 10, and (···) 100 kHz and for $BaTiO_3$ at (——) 1 kHz of (**a**) dielectric constant and (**b**) dielectric loss (98).

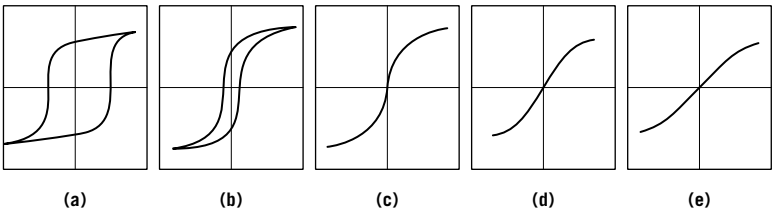

Fig. 12. Dielectric hysteresis in $Pb(Mg_{1/3}Nb_{2/3})O_3$ at (**a**) −150°C; (**b**) −80°C; (**c**) −20°C; (**d**) −10°C; and (**e**) 25°C (98).

transition, and K_{max} decreases and shifts to higher temperatures with increasing measuring frequency. The temperature of the maximum dielectric loss does not coincide with T_{max} in relaxors; rather, the loss increases with measurement frequency. The polarization-electric field behavior exhibits typical ferroelectric hysteresis at temperatures well below the T_{max} as shown in Figure 12. The pronounced hysteresis slowly decays to slim-loop behavior at temperatures above T_{max}. Structural ordering as evidenced by optical anisotropy or x-ray line splitting from optical birefringence and x-ray diffraction studies, respectively, has not been observed in relaxors as in normal ferroelectrics (97).

Relaxor ferroelectrics have been extensively investigated since the late 1970s because of the ability to generate large electrically induced strains, minimal hysteresis of the strain–electric field response, and minimal thermal strain (13,99,100). These materials also show promise in capacitor applications because of large dielectric permittivities (101,102). In addition to actuator and capacitor applications, a large piezoelectric effect can be induced by the application of an external electric field in relaxor ferroelectric materials possessing large polarizations (13). Field-induced piezoelectric transducers exhibit a nonlinear strain–electric field response and are not piezoelectrically active when the external bias is removed. These materials allow for the adjustment (tuning) of the piezoelectric coefficients between on and off states for specific operating conditions. The field-induced piezoelectric and elastic properties of relaxor ferroelectrics have also been investigated for transducer applications, including three-dimensional medical ultrasonic imaging devices.

5.5. Polymer Ferroelectrics. In 1969, it was found that strong piezoelectric effects could be induced in the polymer poly(vinylidene fluoride) (known as PVD_2 or PVDF) by application of an electric field (103). Pyroelectricity, with pyroelectric figures of merit comparable to crystalline pyroelectric detectors (104,105) of PVF_2 films polarized this way, was discovered two year later (106.)

These discoveries were important breakthroughs for the field of electromechanical and pyroelectric devices. Fabrications of an inexpensive, completely flexible, rugged, wide area piezoelectric transducer and pyroelectric detector were realized immediately. Within a few years, a wide variety of prototype devices had been fabricated. These include audio frequency transducers, such as microphones, headphones, and loudspeaker tweeters having excellent frequency response and low distortion because of the low density lightweight transducer film; ultrasonic transducers for underwater applications, such as hydrophones,

and for medical imaging applications; electromechanical transducers for computer and telephone keypads and a variety of other contactless switching applications; and pyroelectric detectors for infrared imaging and intruder detection. At least 1–2 MV/cm of poling field is required to obtain 65 mC/m^2 polarization level of PVDF thin film which is consistent with 50% crystallinity and perfect alignment (107).

6. Economic Aspects

Ferroelectric–polymer composite devices have been developed for large-area transducers, active noise control, and medical imaging applications. North American Philips, Hewlett-Packard, and Toshiba make composite medical imaging probes for in-house use. Krautkramer Branson Co. produces the same purpose composite transducer for the open market. NTK Technical Ceramics and Mitsubishi Petrochemical market ferroelectric–polymer composite materials (108) for various device applications, such as a towed array hydrophone and robotic use. Whereas the composite market is growing with the invention of new devices, total unit volume and dollar amounts are small compared to the ferroelectric capacitor and ferroelectric–piezoelectric ceramic markets (see MEDICAL IMAGING TECHNOLOGY).

Ferroelectric thin films have not, as of this writing, been commercialized. Demand for PTC ferroelectrics has been decreasing rapidly. Wide usage of the fuel injector in automobiles and other types of composite PTC devices is the main reason.

Approximately 40% of the U.S. electronic ceramics industry is represented by ferroelectrics. Table 3 shows U.S. consumption of ceramic capacitors and piezoelectric materials (109).

Japanese suppliers generally dominate the electronic ceramic business. Japanese production of ferroelectric devices in the first nine months of 1990 was valued at $\$711 \times 10^6$ for ceramic capacitors and $\$353 \times 10^6$ for piezoelectric devices, representing growths of 7 and 10.8%, respectively, over the previous year.

Principal producers of ferroelectric capacitors are (110) Murata Manufacturing Co., Ltd., Kyoto, Japan; Kyocera Corp., Kyoto, Japan; Philips Electronics, N.V., Eindhoven, the Netherlands; and NEC Corp., Tokyo, Japan. Principal

Table 3. **U.S. Ceramic Capacitor and Ceramic Piezoelectric Material Consumption**[a]

	Value, $\$ \times 10^6$		
Product	1987	1992	Five-year growth, %
ceramic capacitors[b]	609	740	4
piezoelectric materials	70	115	10

[a]Ref. 109.
[b]Includes chip capacitors.

piezoelectric ceramic component producers are (110) Murata Manufacturing Co., Ltd., Kyoto, Japan; Motorola, Inc., Schaumburg, Ill.; EDO Corp., College Point, N.Y.; Morgan Matroc, Inc., Bedford, Ohio; Kyocera Corp., Kyoto, Japan; and Philips Electronics, N.V., Eindhoven, the Netherlands.

BIBLIOGRAPHY

"Ferroelectrics" in *ECT* 2nd ed., Vol. 9, pp. 1–25, by E. C. Henry, General Electric Co.; in *ECT* 3rd ed., Vol. 10, pp. 1–30, by L. E. Cross, The Pennsylvania State University, and K. H. Härdtl, Philips Forschungslaboratorium Aachen GmbH; in *ECT* 4th ed., Vol. 10, pp. 381–413, by F. X. N. M. Kools and D. Stappels, Philips Components.

CITED PUBLICATIONS

1. M. Faraday, *Experimental Researches in Electricity*, Taylor and Francis, London, 1838; Dover, New York, 1965, Vol. **I**, § 1168.
2. J. Reitz and F. Milford, *Foundations of Electromagnetic Theory*, Addison-Wesley Publishing Co., Inc., Reading, Mass., 1969.
3. J. M. Herbert, *Ceramic Dielectric and Capacitors*, Gordon & Breach, New York, 1985.
4. M. E. Lines and A. M. Glass, *Principles and Applications of Ferroelectrics and Related Materials*, Clarendon, Oxford, UK, 1977.
5. F. Jona and G. Shirane, *Ferroelectric Crystals*, Pergamon Press, Inc., Elmsford, N.Y., 1962.
6. J. Burfoot, *Ferroelectrics, An Introduction to the Physical Principles*, D. Van Nostrand, Princeton, N.J., 1967; R. E. Cohen, *Nature* **358**, 136 (1992).
7. J. F. Nye, *Physical Properties of Crystals*, Clarendon, Oxford, UK, 1957.
8. K. Aizu, *J. Phys. Soc. Jpn.* **20**, 959 (1965); *Phys. Rev.* **146**, 423 (1966).
9. L. A. Shuvalov, *J. Phys. Soc. Jpn.* **285**, 38 (1970).
10. B. Jaffe, W. R. Cooke, Jr., and H. Jaffe, *Piezoelectric Ceramics*, Academic Press, New York, 1971.
11. A. F. Devonshire, *Phil. Mag.* **40**, 1040 (1949) and *Phil. Mag.* **42**, 1065 (1951).
12. Landolt-Börnstein, *Ferroelectric and Anti-ferroelectric Substances*, Vol. **3**, New Series Group III, Springer-Verlag, Berlin, Germany, 1969.
13. S. J. Jang, *Electrostrictive Ceramics for Transducer Applications*, Ph.D. dissertation, The Pennsylvania State University, University Park, 1979.
14. G. H. Haertling and C. E. Land, *J. Am. Ceram. Soc.* **54**, 1 (1971).
15. P. Günter and J. P. Huignard, *Photorefractive Materials and their Applications I, II*, Springer-Verlag, New York, 1988.
16. I. S. Zheludev, *Physics of Crystalline Dielectrics*, Plenum Press, New York, 1971.
17. B. Jaffe, R. S. Roth, and S. Marzullo, *J. Res. Nat. Bur. Stand.* **55**, 239 (1955).
18. E. Sowaguchi, *J. Phys. Soc. Jpn.* **8**, 615 (1953).
19. H. Ouchi, K. Nagano, and S. Hayakawa, *J. Am. Ceram. Soc.* **48**, 630 (1965).
20. H. Ouchi, M. Nishida, and S. Hayakawa, *J. Am. Ceram. Soc.* **49**, 577 (1966).
21. H. Ouchi, *J. Am. Ceram. Soc.* **51**, 169 (1968).
22. Landolt-Börnstein, *Ferroelectric and Anti-ferroelectric Substances*, Vol. 9, New Series Group III, Springer-Verlag, Berlin, Germany, 1977.

23. Landolt-Börnstein, *Ferroelectric and Related Substances*, Vol. **28**, New Series Group III, Springer-Verlag, Berlin, Germany, 1990.
24. J. M. Herbert, *Ferroelectric Transducers and Sensors*, Gordon & Breach, New York, 1982.
25. A. J. Moulson and J. M. Herbert, *Electroceramics*, Chapman and Hall, London, 1990.
26. J. H. Adair, D. A. Anderson, G. O. Dayton, and T. R. Shrout, *J. Mater. Educ.* **9**, 71–118 (1987).
27. S. B. Krupanidhi, *J. Vac. Sci. Tech.* **A10**, 1509 (1992).
28. M. H. Francombe and S. V. Krishnaswamy, *J. Vac. Sci. Tech.* **A8**, 1382 (1990).
29. J. F. Scott and C. A. Araujo, *Science* **246**, 14800 (1989).
30. L. E. Sanchez, S. Y. Wu, and I. K. Naik, *Appl. Phys. Lett.* **56**, 2399 (1990).
31. S. B. Krupanidhi, N. Maffei, M. Sayer, and K. El-Assal, *J. Appl. Phys.* **54**, 6601 (1983).
32. M. Okuyama and Y. Hamakawa, *Ferroelectrics* **63**, 243 (1985).
33. S. B. Krupanidhi and M. Sayer, *J. Vac. Sci. Technol.* **A2**, 203 (1984).
34. K. Sreenivas and M. Sayer, *J. Appl. Phys.* **64**, 1484 (1988).
35. R. N. Castellano and L. G. Feinstein, *J. Appl. Phys.* **50**, 4406 (1979); S. B. Krupanidhi, H. Hu, and V. Kumai, *J. Appl. Phys.* **71**, 376 (1992).
36. D. Xiao, Z. Xiao, J. Zhu, Y. Li, and H. Guo, *Ferroelectrics* **108**, 59 (1990).
37. R. Ramesh and co-workers, *Appl. Phys. Lett.* **57**, 1505 (1990).
38. S. B. Krupanidhi and co-workers, *J. Vac. Sci. Tech.*, **A10**, 1815 (1992).
39. K. L. Saenger, R. A. Roy, K. F. Etzold, and J. J. Cuomo, *Mater. Res. Soc. Symp. Proc.* **200**, 115 (1990).
40. M. Okuyama, Y. Togani, and Y. Hamakawa, *Appl. Surf. Sci.* **33/34**, 625 (1988).
41. Y. Masuda, A. Baba, H. Masomoto, T. Goto, M. Minikata, and T. Kirai, in Ref. 9, p. 337.
42. W. T. Petusky and S. K. Dey in *Proceedings of the 3rd International Symposium on Integrated Ferroelectrics, Colorado Springs, Colo., Apr. 1991*, Gordon and Breach Science Publishers, New York (in press).
43. K. D. Budd, S. K. Dey, and D. A. Payne, *Br. Ceram. Proc.* **36**, 107 (1985).
44. S. K. Dey and R. Zuleeg, *Ferroelectrics* **108**, 37 (1990).
45. G. A. C. M. Spierings, M. J. E. Ulenaers, G. L. Kampschoer, H. A. M. van Hal, and P. K. Larsen, *J. Appl. Phys.* **70**, 2290 (1991).
46. R. W. West, *Ferroelectrics* **102**, 53 (1990).
47. G. H. Haertling, *J. Vac. Sci. Technol.* **A9**, 414 (1976).
48. M. Iukawa and K. Toda, *Appl. Phys. Lett.* **29**, 491 (1976).
49. A. Mansingh and S. B. Krupanidhi, *J. Appl. Phys.* **51**, 5408 (1980).
50. J. R. Slack and J. C. Burfoot, *Thin Solid Films* **6**, 233 (1970).
51. A. Mansingh and S. B. Krupanidhi, *Thin Solid Films* **80**, 359 (1981).
52. J. Kojima, M. Okuyama, T. Nakagawa, and Y. Hamakawa, *Jpn. J. Appl. Phys.* **22**, Suppl. 2, 14 (1983).
53. M. Okada, S. Takai, M. Amemiya, and K. Tominaga, *Jpn. J. Appl. Phys.* **28**, 1030 (1989).
54. P. C. Van Buskirk, R. Gardiner, P. S. Kirlin, and S. B. Krupanidhi, *J. Vac. Sci. Technol.* (in press).
55. S. Sinharoy, H. Buhay, M. H. Francombe, W. J. Takei, N. J. Doyle, J. R. Rieger, D. R. Lampe, and E. Stepke, *J. Vac. Sci. Technol.* (in press).
56. H. Adachi, T. Mitsuyu, O. Yamazaki, and K. Wasa, *J. Appl. Phys.* **60**, 736 (1986).
57. J. J. Cuomo, S. M. Rossnagel and H. R. Kaufman, *Handbook of Ion Beam Processing Technology*, Noyes, Park Ridge, N.J., 1989.
58. R. K. Singh and J. Narayou, *Phys. Rev.* **B42**, 8843 (1990).

59. D. B. Beach, *IBM J. Res. Dev.* **34**, 795 (1990).
60. R. E. Newnham, D. P. Skinner, and L. E. Cross, *Mater. Res. Bull.* **13**, 525 and 599 (1978).
61. K. A. Klicker, J. V. Biggers, and R. E. Newnham, *J. Am. Ceram. Soc.* **64**, 5 (1981).
62. M. J. Haun, P. Moses, T. R. Gururaja, and W. A. Schulze, *Ferroelectrics* **49**, 259 (1983).
63. K. Rittenmyer, T. Shrout, W. A. Schulze, and R. E. Newnham, *Ferroelectrics* **41**, 189 (1982).
64. A. Safari, R. E. Newnham, L. E. Cross, and W. A. Schulze, *Ferroelectrics* **41**, 197 (1982).
65. R. E. Newnham, L. J. Bowen, K. A. Klicker, and L. E. Cross, *Mater. Eng.* **112**, 93 (1980).
66. J. Runt and E. C. Galgoci, *J. Appl. Polym. Sci.* **39**, 611 (1984).
67. T. R. Gururaja, W. A. Schulze, L. E. Cross, R. E. Newnham, B. A. Auld, and J. Wang, *IEEE Trans. Sonic Ultrasonics* **SU-32**, 481 and 499 (1985).
68. J. R. Giniewicz, R. E. Newnham, A. Safari, and D. Moffatt, *Ferroelectrics* **73**, 405–417 (1987).
69. S. Sa-Gong, A. Safari, S. J. Jang, and R. E. Newnham, *Ferroelectric Lett.* **5**, 131 (1986).
70. K. A. Hu, J. Runt, A. Safari, and R. E. Newnham, *Ferroelectrics* **68**, 115 (1986).
71. W. R. Buessem, L. E. Cross, and A. K. Goswami, *J. Am. Ceram. Soc.* **49**, 33 (1966).
72. J. Van Kanderaat and R. E. Setterington, *Piezoelectric Ceramics, Application Book*, Ferroxcube Corp., New York, 1974.
73. N. W. Hagood, E. F. Crawley, J. deLuis, and E. H. Anderson, in C. A. Rogers, ed., *Smart Materials, Structures, and Mathematical Issues*, Technomic Publishing Co., Lancaster, Pa., 1988, p. 80.
74. L. M. Levinson, *Electronic Ceramics*, Marcel Dekker, New York, 1988.
75. K. Hikita, K. M. Nichioka, and M. Ono, *Ferroelectrics* **49**, 265 (1983).
76. R. Y. Ting, A. Halliyal, and A. S. Bhalla, *Jpn. J. Appl. Phys.* **24** (Suppl. 24-2), 982 (1985).
77. A. Halliyal, A. Safari, A. S. Bhalla, R. E. Newnham, and L. E. Cross, *J. Am. Ceram. Soc.* **67**, 331 (1984).
78. K. A. Klicker, W. A. Schulze, and J. V. Biggers, *J. Am. Ceram. Soc.* **65**, C208 (1982).
79. H. P. Savakus, K. A. Klicker, and R. E. Newnham, *Mater. Res. Bull* **16**, 677 (1981).
80. N. M. Shorrocks, M. E. Brown, R. W. Whatmore, and F. W. Ainger, *Ferroelectrics* **54**, 215 (1984).
81. M. Kahn, R. W. Rice, and D. Shadwell, *Advan. Ceram. Mater.* **1**, 55 (1986).
82. S. Pilgrim and R. E. Newnham, "A New Type of 3-0 Composites," presented at the *American Ceramics Society, Electronics Division 86 Meeting*, Chicago, 1986.
83. T. R. Shrout, L. J. Bowen, and W. A. Schulze, *Mater. Res. Bull.* **15**, 1371 (1980).
84. A. Safari, A. Halliyal, R. E. Newnham, and I. M. Lachman, *Mater. Res. Bull.* **17**, 301 (1982).
85. L. A. Pauer, *IEEE Intl. Conv. Rec.* 1 (1973).
86. H. Banno and S. Saito, *Jpn. J. Appl. Phys.* **22** (Suppl. 22-2), 67 (1983).
87. R. Y. Ting, "Evaluation of New Piezoelectric Composite Materials for Hydrophone Applications," presented at the *Bernard Jaffe Memorial Colloquium*, American Ceramics Society, 86 Meeting, Pittsburgh, 1984.
88. D. L. Monroe, J. B. Blum, and A. Safari, *Ferroelectrics Lett.* **5**, 39 (1986).
89. T. R. Gururaja and co-workers, *Ferroelectrics* **39**, 1245 (1981).

90. W. A. Smith, A. A. Shaulov, and B. M. Singer in *Proceedings of the 1984 IEEE Ultrasonics Symposium*, Dallas, Tex., 1984, p. 539.
91. A. A. Shaulov, W. A. Smith, and B. M. Singer, in Ref. 90, p. 545.
92. W. A. Smith, A. Shaulov, and B. A. Auld in *Proceedings of the 1985 IEEE Ultrasonics Symposium*, San Francisco, Calif., 1985, p. 642.
93. A. A. Shaulov and W. A. Smith, in Ref. 92, p. 648.
94. H. Takeuchi, C. Nakaya, and K. Katakura in Ref. 90, p. 504.
95. H. Takeuchi and C. Nakaya, *Ferroelectrics* **68**, 53 (1986).
96. A. Fukumoto, *Ferroelectrics* **40**, 217 (1982).
97. L. E. Cross, *Ferroelectrics* **76**, 241–267 (1987).
98. T. R. Shrout and J. P. Dougherty, *Ceram. Trans.* **8**, 3–19 (1990).
99. J. Kuwata, K. Uchino, and S. Nomura, *Jpn. J. Appl. Phys.* **19**, 2099 (1980).
100. S. Nomura and K. Uchino, *Ferroelectrics* **41**, 117 (1982); **50**, 197 (1983).
101. S. L. Swartz and co-workers, *J. Am. Ceram. Soc.* **67**, 311 (1984).
102. T. R. Shrout and A. Halliyal, *Am. Ceram. Bull.* **66**, 704 (1987).
103. H. Kawai, *Jpn. J. Appl. Phys.* **8**, 975 (1969).
104. J. G. Bergman, J. H. McFee, and G. R. Crane, *Appl. Phys. Lett.* **18**, 203 (1971).
105. K. Nakamura and Y. Wada, *J. Polym. Sci.* **A-29**, 161 (1971).
106. A. M. Glass, J. H. McFee, and J. G. Bergman, *J. Appl. Phys.* **42**, 5219 (1971).
107. T. T. Wang, J. M. Herbert, and A. M. Glass, *The Applications of Ferroelectric Polymers,* Blackie & Sons, Ltd., London, 1988.
108. H. Banno and K. Ogura, *J. Ceram. Soc. Jpn.* **100**, 551 (1992).
109. T. J. Dwyer and R. B. McPhillips, *Ceram. Bull.* **67**, 1894 (1988).
110. *Ceram. Ind.*, Jul. 1988, June 1991, Aug. 1992.

SEI-JOO JANG
The Pennsylvania State University